the plant journal

SEB SOCIETY FOR EXPERIMENTAL BIOLOGY

The Plant Journal (2023) **114,** 683–698 doi: 10.1111/tpj.16166

FaMYB123 interacts with FabHLH3 to regulate the late steps of anthocyanin and flavonol biosynthesis during ripening

Félix J. Martínez-Rivas[1,2,†], Rosario Blanco-Portales[1], María P. Serratosa[3], Pablo Ric-Varas[4], Víctor Guerrero-Sánchez[1,‡], Laura Medina-Puche[1,5], Lourdes Moyano[3], José A. Mercado[4], Saleh Alseekh[2,6], José L. Caballero[1], Alisdair R. Fernie[2,6], Juan Muñoz-Blanco[1,*,¶] and Francisco J. Molina-Hidalgo[1,*,¶]

[1]*Department of Biochemistry and Molecular Biology, University of Cordoba, Edificio Severo Ochoa, Campus de Rabanales, E-14014, Córdoba, Spain,*

[2]*Max-Planck-Institute of Molecular Plant Physiology, Am Mühlenberg 1, 14476, Potsdam-Golm, Germany,*

[3]*Department of Agricultural Chemistry, University of Cordoba, Edificio Marie Curie, Campus de Rabanales, E-14014, Córdoba, Spain,*

[4]*Department of Plant Biology, Instituto de Hortofruticultura Subtropical y Mediterránea La Mayora, University of Málaga, Campus de Teatinos, E-29071, Málaga, Spain,*

[5]*Department of Plant Biochemistry, Centre for Plant Molecular Biology (ZMBP), Eberhard Karls University, Tübingen, Germany,*

[6]*Center of Plant Systems Biology and Biotechnology, Ruski Blvd. 139, Plovdiv 4000, Bulgaria*

Received 11 March 2022; accepted 17 February 2023; published online 24 February 2023.

*For correspondence (e-mail bb1mublj@uco.es; b52mohif@uco.es)

[¶]Both authors have contributed equally to this paper.

[†]Present address: Centro de Biotecnología y Genómica de Plantas, Universidad Politécnica de Madrid (UPM) - Instituto Nacional de Investigación y Tecnología Agraria y Alimentaria (INIA-CSIC), Madrid, Spain

[‡]Present address: Vascular Pathophysiology Area, Cardiovascular Proteomics Laboratory, Centro Nacional de Investigaciones Cardiovasculares Carlos III (CNIC), 28029, Madrid, Spain

SUMMARY

In this work, we identified and functionally characterized the strawberry (*Fragaria* × *ananassa*) R2R3 MYB transcription factor FaMYB123. As in most genes associated with organoleptic properties of ripe fruit, FaMYB123 expression is ripening-related, receptacle-specific, and antagonistically regulated by ABA and auxin. Knockdown of FaMYB123 expression by RNAi in ripe strawberry fruit receptacles downregulated the expression of enzymes involved in the late steps of anthocyanin/flavonoid biosynthesis. Transgenic fruits showed a parallel decrease in the contents of total anthocyanin and flavonoid, especially malonyl derivatives of pelargonidin and cyanidins. The decrease was concomitant with accumulation of proanthocyanin, propelargonidins, and other condensed tannins associated mainly with green receptacles. Potential coregulation between FaMYB123 and FaMYB10, which may act on different sets of genes for the enzymes involved in anthocyanin production, was explored. FaMYB123 and FabHLH3 were found to interact and to be involved in the transcriptional activation of *FaMT1*, a gene responsible for the malonylation of anthocyanin components during ripening. Taken together, these results demonstrate that FaMYB123 regulates the late steps of the flavonoid pathway in a specific manner. In this study, a new function for an R2R3 MYB transcription factor, regulating the expression of a gene that encodes a malonyltransferase, has been elucidated.

Keywords: strawberry, *Fragaria*, fruit, ripening, transcription factor, malonyltransferase, MYB, anthocyanin/flavonoid biosynthesis, phenylpropanoid.

INTRODUCTION

Strawberry (*Fragaria* × *ananassa* Duch. cv. Camarosa) fruits contain various nutritive bioactive compounds (sugars, vitamins, minerals) and non-nutritive bioactive compounds (flavonoids, anthocyanins, phenolic acids). Also, they have a pleasant taste and flavor, making strawberry one of the most widely appreciated fruits. These types of compounds have been related to the promotion of human health and also to the prevention of degenerative and metabolic diseases (Giampieri et al., 2015). Especially well known among them are

phenolics, which exhibit potent antioxidant and anti-inflammatory activities (Wang et al., 1996). Flavonoids (particularly anthocyanins), which are the most abundant polyphenols in strawberry, occur mainly as pelargonidin and cyanidin derivatives, followed by ellagitannins, flavonols, flavanols, and phenolic acids (Giampieri et al., 2012; Giampieri et al., 2014; Giampieri et al., 2015).

Most of these compounds are synthesized during ripening as a strategy to attract predators to eat the fruits and spread seeds. The anthocyanins identified to date in strawberry include the 3-glucosides and 3-rutinosides of cyanidin and pelargonidin and two acylated derivatives of pelargonidin (viz., 3-(malonyl) glucoside and 3-(6-acetyl)-glucoside) (Wu & Prior, 2005). Small amounts of flavanol–anthocyanin complexes consisting of pelargonidin 3-glucoside connected to catechin, epicatechin, afzelechin, and epiafzelechin via $\alpha 4 \rightarrow 8$ linkages have also been found (Fossen et al., 2004). Anthocyanin compositions vary between cultivars (Aaby et al., 2012). Pelargonidin-3-glucoside, which is the main compound responsible for its red color (Aaby et al., 2005; Wang et al., 2002; Wang & Zheng, 2001), is the most abundant anthocyanin, contributing 60–95% to the total anthocyanin content. Pelargonidin-3-malonylglucoside has been identified as the second most abundant anthocyanin, accounting for 0 to 33.5%, depending on the cultivar (Aaby et al., 2012).

Ripening in strawberry is regulated by a number of transcription factors (TFs), including MYBs, which are a large family whose members occur in all eukaryotic organisms and have one or more repeats of the MYB domain (Kranz et al., 2000; Lipsick, 1996). R2R3 MYBs can be recognized by their two imperfect MYB repeats following R2 and R3 structures in c-MYB (Kranz et al., 2000). To play their regulatory roles, MYB TFs interact with other TFs and proteins involved in transcription processes. For example, the formation of an MBW complex, consisting of MYB and basic helix–loop–helix (bHLH) TFs in combination with WD40 proteins, is important for targeting the promoters of genes involved in various metabolic and developmental pathways such as flavonoid accumulation, glucosinolate production, and trichome generation (Matias-Hernandez et al., 2017; Xie et al., 2016; Xu et al., 2015). The ability of MYB–bHLH complexes to recognize some *cis*-elements on the promoter of regulated genes ensures specificity to the target gene (Bemer et al., 2017; Lai et al., 2014).

The roles of some MYB and bHLH genes in strawberry have been elucidated. For example, FaMYB1 is a repressor of structural genes of the phenylpropanoid/flavonoid/anthocyanin pathway (Aharoni et al., 2001). Also, FaMYB10 is involved the biosynthesis of these compounds in ripe receptacles. FaMYB10 activates structural genes of the pathway in ripe fruit receptacles (An et al., 2015; Lin-Wang et al., 2010; Medina-Puche et al., 2014). Moreover, FaMYB9/FaMYB11, FabHLH3, and FaTTG1 have been deemed positive regulators of the biosynthesis of proanthocyanidins, which are the main flavonoids produced by unripe strawberry (Schaart et al., 2013).

We used transcriptomic analyses to identify a ripening-related R2R3 MYB TF (FvH4_5g32460), hereinafter FaMYB123, which exhibits a well-defined fruit-specific, ripening-related expression pattern (Medina-Puche et al., 2016). Molecular and physiological studies have shown this TF to be involved in the regulation of structural genes in the late steps of the production of anthocyanins or flavonols, which are specialized metabolites accumulating in ripe fruit receptacles. As shown here, FaMYB123 regulates a gene that encodes a malonyltransferase, which is involved in the biosynthesis of cyanidin and pelargonidin malonyl derivatives – the second most abundant group of compounds in ripe receptacles (Aaby et al., 2012).

RESULTS

Previous transcriptomic studies allowed us to select a group of genes for further functional characterization (Medina-Puche et al., 2016). Among the TFs identified, only three MYB-type TFs were upregulated in red ripe receptacles and regulated positively by ABA and negatively by auxins, which suggested that they were involved in different ripening-related processes in fruit receptacles. These three TFs were FaMYB10 (FvH4_1g22020), FaEOBII (FvH4_6g50930), and FaMYB123 (FvH4_5g32460). FaMYB10 and FaEOBII were previously characterized by Medina-Puche et al. (2014, 2015), who demonstrated the central role played by both TFs in controlling major processes of flavonoid/phenylpropanoid metabolism during ripening. In this work, we addressed the functional characterization of the MYB TF FaMYB123 (FvH4_5g32460), whose expression pattern suggests that it might regulate the expression of some major genes involved in strawberry ripening.

FaMYB123 encodes an R2R3 MYB TF located in the nucleus

The putative sequence of the predicted R2R3 MYB gene *FvH4_5g32460* was used to design specific primers for open reading frame (ORF) amplification by PCR with cDNA from red fruits. Sequencing analysis of the resulting PCR product showed that the amplicon was shorter than the predicted sequence in the Genome Database for Rosaceae (Figure S1a). *In silico* analysis of the deduced FaMYB123 protein revealed the presence of the characteristic R2R3 DNA-binding motifs at the N-terminus (Figure S1b).

A full-length MYB phylogenetic tree with predicted proteins from strawberry and *A. thaliana* was generated. FaMYB123 shows the highest homology with transparent testa 2 (AtTT2) (Figure S2) (Kranz et al., 1998). A more detailed phylogenetic analysis with other transparent testa homologs with inferred function showed FaMYB123 to be a close homolog of VvMYBPA2, DkMYB2, AcMYB123, and

MdMYB9, which are related to proanthocyanidin and anthocyanin production (An et al., 2015; Appelhagen et al., 2011; Terrier et al., 2009; Wang et al., 2019) (Figure 1a). FaMYB123 contains the conserved motif (D/E)LX_2(R-K)$X_3LX_6LX_3R$ in its protein sequence (Figure S3a). This domain confers the ability to bind to bHLH TFs. The motif has also been found in FaMYB123 orthologs, and some have been found to bind to bHLH TFs such as AtTT2, DkMYB2, and AcMYB123 (Appelhagen et al., 2011; Wang et al., 2019; Xu et al., 2021). Motif analysis was performed with the FabHLH3 protein sequence, which is a well-known regulator of proanthocyanidin production. FabHLH3 falls in subgroup IIIf of the bHLH TFs (Schaart et al., 2013); it possesses an N-terminal MYB DNA-interacting region with conserved motifs and a C-terminal bHLH structure (Figure S3b).

The subcellular location of the TF was determined by confocal microscopy. A GFP-FaMYB123 fusion protein was transiently expressed under control of the 35S promoter in *Nicotiana benthamiana* leaves. Fluorescence was only detected in the nucleus and colocalized with the nuclear marker DAPI (Figure 1b), which confirmed the nuclear bioinformatic prediction (Figure S1c). Therefore, FaMYB123 is located in the nucleus.

FaMYB123 is strongly expressed in receptacles and hormonally regulated throughout strawberry fruit growth and ripening

We conducted quantitative real-time PCR (qRT-PCR) analysis to examine the spatiotemporal gene expression pattern of *FaMYB123* and its response to ABA and auxins, the main hormones governing ripening in strawberry fruit. *FaMYB123* is lowly expressed during growth of the fruit receptacle (G1, G3, and W), but markedly upregulated at the ripening and senescence stages (R, OR, and SE), and it peaks at the OR stage (Figure 2a). *FaMYB123* expression in other plant tissues such as runners, leaves, flowers, and petals was low relative to that in ripe fruits (Figure 2b). Also, *FaMYB123* expression in achenes was negligible (Figure 2c). Taken together, these results suggest that FaMYB123 regulates specific ripening-related physiological processes occurring in the receptacle.

Most of the ripening-related genes associated with the sensory properties and quality of strawberry are antagonistically regulated by both auxins, synthetized in achenes, and ABA (Medina-Puche et al., 2016). The potential effect of ABA on *FaMYB123* expression was examined in two assays in which the ABA content was reduced by inhibiting the enzymatic activity of FaNCED1. In the first assay, the synthetic inhibitor nordihydroguaiaretic acid (NDGA) was injected, and in the second assay, *FaNCED1* was knocked down by RNAi. A concomitant decrease in *FaMYB123* expression and ABA content was observed (Figure 3a,b). These assays were supplemented with one involving accumulation of ABA by effect of water stress. A significant increase in *FaMYB123* expression was found to correlate with an also increased ABA content in stressed fruits, indicating that *FaMYB123* transcription is regulated by this hormone (Figure 3c). The effect of auxins was examined by comparing *FaMYB123* expression in receptacles 5 days after removal of achenes – the source of auxins – which revealed increased expression (Figure 3d); however, externally applied indole-3-acetic acid (IAA) abolished this inductive effect. These results demonstrate that auxins negatively regulate *FaMYB123* expression. Altogether, they show that, as with other TFs altering organoleptic properties during strawberry ripening (Medina-Puche et al., 2015; Molina-Hidalgo et al., 2017), *FaMYB123* expression is regulated by ABA and auxin levels in fruit receptacles.

Metabolite analysis of FaMYB123-RNAi in transgenic fruits

The role of FaMYB123 in the ripening process was examined by generating transgenic plants to knock down its expression. The degree of silencing was assessed in transgenic receptacles. *FaMYB10* expression levels were determined as an indicator of the ripening stage (Figure S4). Lines 28, 31, and 32 were selected for further analysis as they exhibited the lowest expression (below 10%) relative to control receptacles transformed with the empty vector. As noted earlier, FaMYB123 bears high sequence homology with other MYB TFs related to proanthocyanidin and anthocyanin production in fruits (Figure 1a).

As can be seen from Figure 4(a), the total anthocyanin content of transgenic ripe receptacles was significantly decreased. This result clearly shows that FaMYB123 is involved in anthocyanin production. UPLC-MC was used to identify in greater detail the major soluble phenolic compounds involved in the flavonoid/phenylpropanoid pathway. Principal component analysis of the identified specialized metabolites clearly separated transgenic and control receptacles (Figure 4b). Thus, transgenic receptacles had lower concentrations of pelargonidin-3-glucoside and a virtually complete loss of pelargonidin-3-(6′-malonylglucoside), a pelargonidin-3-glucose derivative (Figure 4c and Table S1). There was also a decrease in other pelargonidin derivatives, such as pelargonidin-3-rutinoside and pelargonidin-3,5-diglucoside, and a concomitant decrease in cyanidins including cyanidin-3-glucoside and cyanidin-3-rutinoside. As with pelargonidin, the malonyl derivative cyanidin-3-(6′-malonylglucoside) was nearly absent from transgenic receptacles, which suggests that FaMYB123 plays a specific role in regulating production of malonyl derivatives (Figure 4c, Table S1). Flavonol and flavone levels were also determined. The main flavonol in strawberry, kaempferol, and its derivatives kaempferol-3-glucose, kaempferol-3-rutinoside, and kaempferol-3-malonylglucose were less abundant in

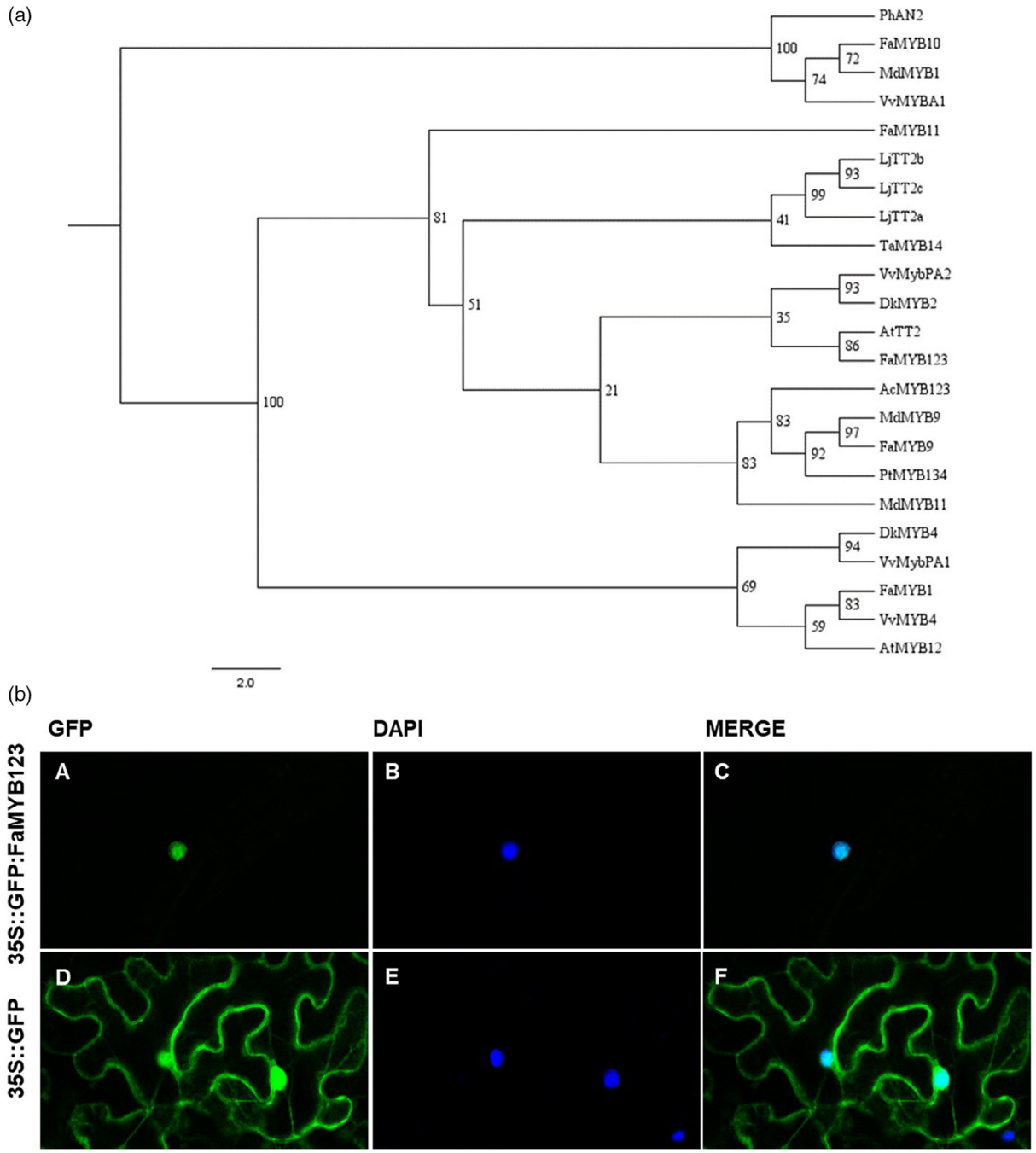

Figure 1. (a) Phylogenetic tree of FaMYB123 and its known R2R3 MYB transcription factors. The tree was constructed with the software FigTree, using the neighbor joining method with 1000 bootstrap replicates. Numbers next to each node represent confidence percentages. The GenBank accession numbers are FaMYB123 (MW081987), LjTT2a (AB300033.2), LjTT2b (AB300034.2), LjTT2c (AB300035.1), TaMYB14 (JN049641.1), PtMYB134 (FJ573151.1), PhAN2 (AF146702.1), MdMYB1 (DQ886414.1), AtTT2 (NP_198405.1), VvMybPA1 (AM259485.1), FaMYB10 (EU155162.1), VvMYBPA2 (EU919682.1), DkMYB2 (AB503699.1), AcMYB123 (MH643775), DkMYB4 (AB503701.1), AtMYB12 (DQ224277.1), VvMYB4 (EF113078.1), FaMYB1 (AF401220.1), MdMYB11 (AAZ20431), FaMYB11 (AFL02461), FaMYB9 (AFL02460), MdMYB9 (ABB84757), VvMYBA1 (AB097923.1), and VvMYBA2 (AB097924.1). (b) Subcellular localization of FaMYB123 in *Nicotiana benthamiana* leaves. The leaves were agroinfiltrated with translational constructs 35S::GFP:FaMYB123 and with 35S::GFP as control. (a, c) Leaves infiltrated with *Agrobacterium* carrying plasmid 35S::GFP:FaMYB123. (d, f) Leaves infiltrated with 35S::GFP (d and f). GFP, green fluorescent protein; DAPI, 4′,6-diamidino-2-phenylindole (nucleic dye); MERGE, merged view of GFP and DAPI images.

transgenic receptacles than in control receptacles. Quercetins exhibited the same pattern as quercitin-3-glucose and quercitin-3-malonylglucose, which were present in decreased amounts in transgenic fruits, and so did the flavonoid quercitin-3-rutinoside (rutin), whose levels were also lower (Figure 4c, Table S1).

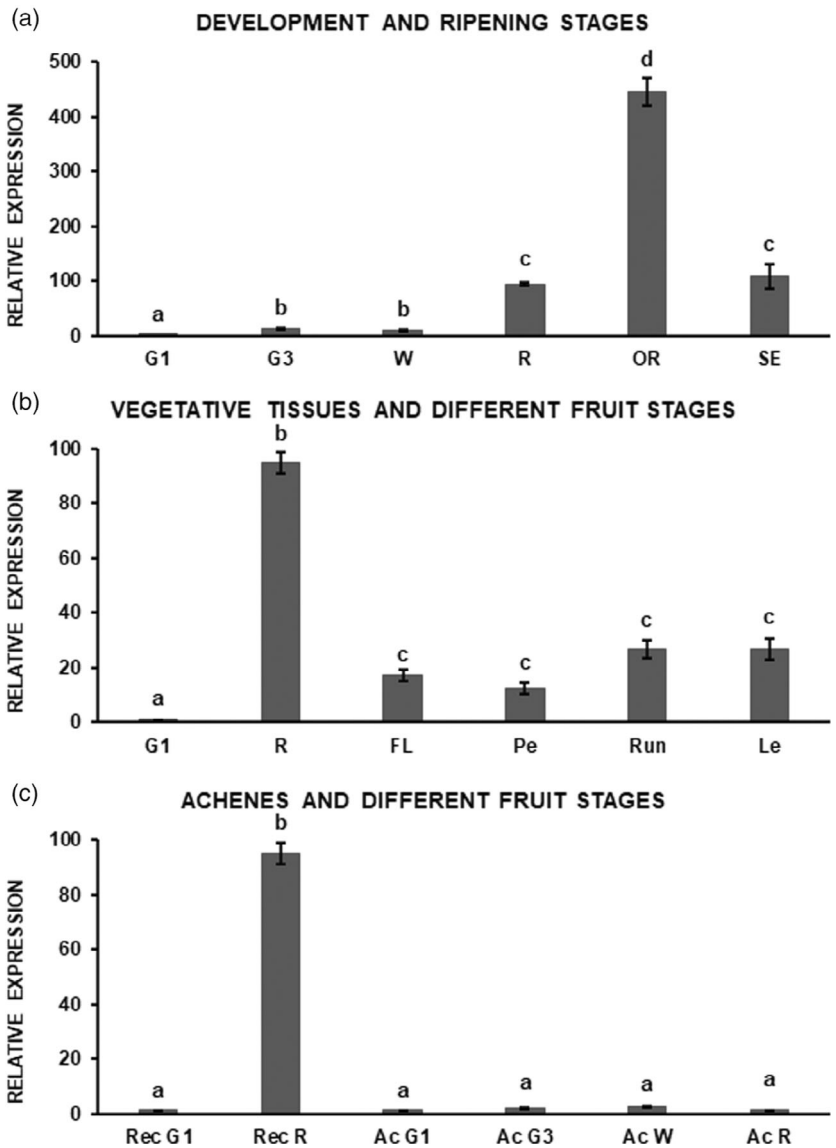

Figure 2. (a) Developmental expression of strawberry *FaMYB123* in fruit receptacles. (b) Vegetative tissues versus G1 and red receptacles. (c) Achenes versus G1 and red receptacles of *Fragaria* × *ananassa* cv. Camarosa. qRT-PCR results were obtained by using specific primers *FaMYB123*. Quantification was based on Ct values. mRNA levels were normalized to the receptacle G1 value in all experiments. Mean values ± SD of five independent experiments are shown. G1, small-sized green fruit; G3, full-sized green fruit; W, white stage; R red stage; OR, overripe stage; SE, senescent stage; REC G1, receptacle G1; REC R, receptacle R; FL, flower; Pe, petal; Run, runner; Le, leaf; Ac G1, achenes in small-sized green fruits; Ac G3, achenes in full-sized green fruits; Ac W, achenes at the white stage; Ac R, achenes at the red stage. Statistical significance was determined by one-way ANOVA. Letters indicate significant differences ($P < 0.05$) as per Scheffe's post-hoc test.

Increased levels of propelargonidins and procyanidins, which are dimers and trimers of pelargonidin and cyanidin, respectively, were found, and so were increased contents of (epi)catechin and (epi)afzelechin (Figure 4c, Table S1). Also, epi(catechin), sanguiin, and ellagic acids were present at increased levels in transgenic receptacles, leading to over-accumulation of condensed aggregates and tannins, which are usually present at low levels in ripe receptacles. This misbalance may have resulted from the metabolic flux in transgenic fruits being redirected in response to downregulation of FaMYB123-controlled enzymes.

FaMYB123 partially regulates anthocyanin and flavonol metabolic pathways

The decreased levels of anthocyanins found in FaMYB123-RNAi fruits (Figure 4a) led us to conduct qRT-PCR analysis to determine the transcript levels of the genes involved in flavonoid/phenylpropanoid metabolism. FaMYB123 seems to be specific to the late steps of the phenylpropanoid pathway. Expression of the early genes *FaPAL*, *FaDFR*, *FaCHS*, *FaCHI*, *FaCAD*, and *FaCCR* was not different in transgenic receptacles, but *FaC4H* and *Fa4CL*

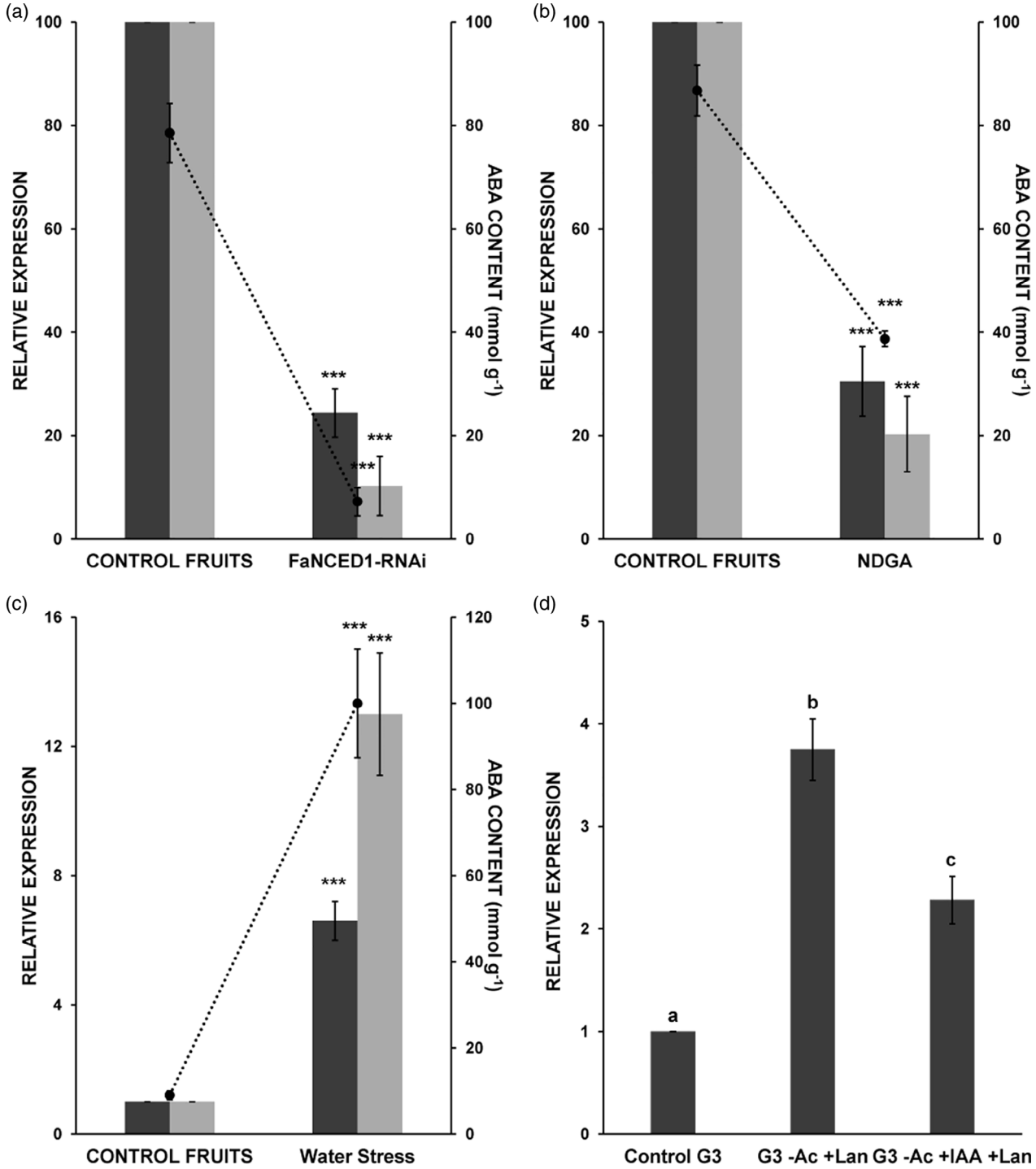

Figure 3. qRT-PCR analysis of *FaMYB123* and *FaNCED1* gene expression in (a) strawberry G-W fruits agroinfiltrated with the NCED1-RNAi construct, (b) G-W fruits treated with NDGA, and (c) strawberry G-W fruits under water stress. The dashed lines represent ABA contents in the fruits. (a) Control fruits, strawberry fruits infiltrated with empty pFRN vector; NCED1-RNAi fruits, transgenic strawberry fruits agroinfiltrated with the FaNCED1-pFRN construct. (b) Control fruits, G-W fruits injected with H_2O; NDGA, G-W fruits injected with NDGA (100 μM), with both samples harvested 8 days after the beginning of treatment. (c) Control fruits, fruits with their pedicels immersed in Murashige–Skoog medium containing sucrose. Gene expression of *FaMYB123* and *FaNCED1* was analyzed in fruits with their pedicels kept in the air. (d) qRT-PCR analysis of the effects of removing achenes from G3 developing fruits and their treatment with auxins on *FaMYB123* gene expression. After auxin treatment, mRNA levels were normalized to G3 fruit (control). Control G3, middle-sized green fruit receptacle; G3 − Ac + Lan, G3 fruit receptacle without achenes for 5 days and covered with lanolin; G3 − Ac + IAA + Lan, G3 fruit receptacle without achenes plus IAA, diluted in lanolin, for 5 days (added on day 0). The cultivar used was *Fragaria* × *ananassa* cv. Elsanta. Mean values ± SD of five independent experiments are shown. Statistical significance was determined by Student's *t*-test. ***$P < 0.001$. Gray bars, *FaNCED1*; black bars, *FaMYB123*; lines, ABA content.

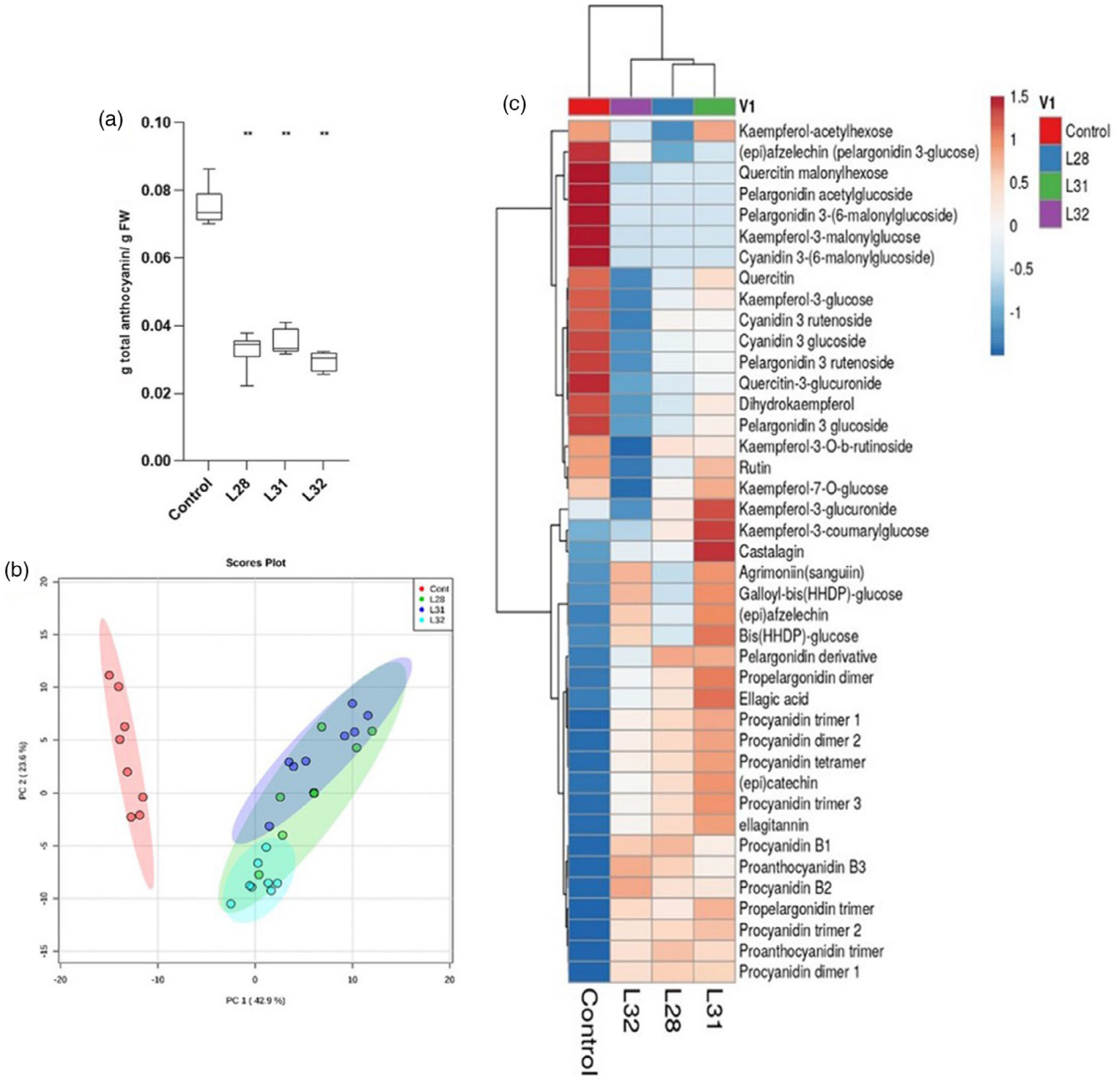

Figure 4. (a) Quantification of anthocyanin in control and FaMYB123-RNAi red receptacles (values obtained from absorbance measurements at 515 nm). (b) Principal component analysis of metabolites identified in receptacles of control samples (red dots) versus transgenic lines (green, blue, and cyan dots). Eight replicates were used in the metabolomic analysis under each condition. (c) Heatmap for secondary metabolism profiling by LC-MS analysis. Extracted anthocyanins, flavonols, procyanidin, and proanthocyanidins and condensed tannins. On the color scale on the right, red represents high contents and blue represents low contents.

exhibited slightly increased levels (Figure 5a). A clear reduction of genes involved in anthocyanin biosynthesis was found, including *FaANS1* and *FaGT1*, which encode key enzymes in this pathway and have been demonstrated to be responsible for the content of pelargonidin-3-glucose (Griesser et al., 2008). Additionally, we explored the possible coregulation between FaMYB123 and FaMYB10, which has been described as a master regulator of this pathway (Medina-Puche et al., 2014). Knockdown of *FaMYB10* resulted in a general downregulation of the structural pathway (Figure 5).

Based on the decreased levels of malonyl derivatives found in transgenic fruits, we delved into the last step of the phenylpropanoid pathway. Up to seven malonyltransferases have been linked to the production of pelargonidin-3-(6′-malonylglucoside) in strawberry (Davik et al., 2020). We examined their expression patterns and identified *FaMT1* and *FaMT5* as ripening- and fruit-specific (Figure S5a). Both

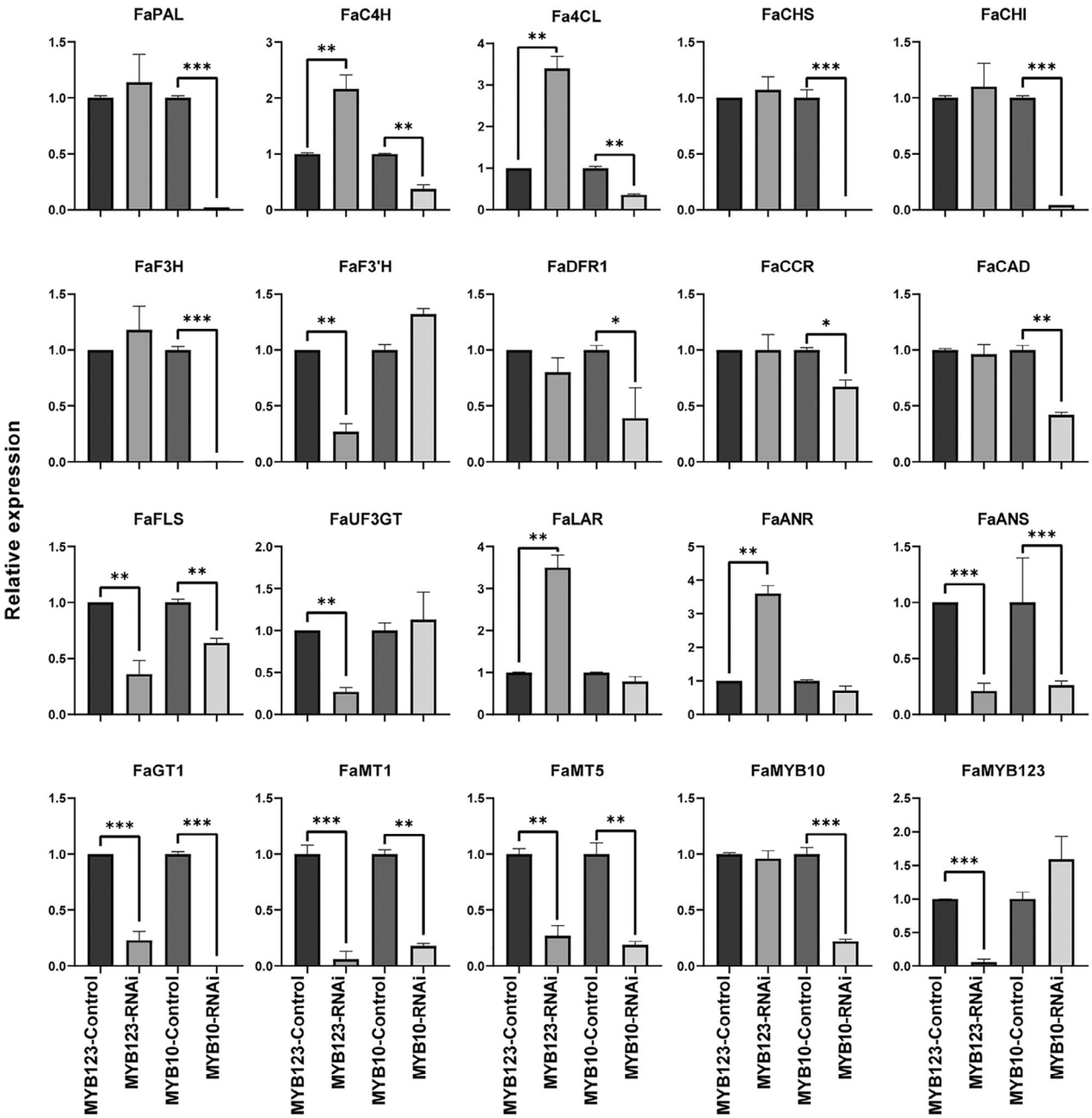

Figure 5. Expression of selected genes related to phenylpropanoid and flavonoid metabolism in FaMYB123-RNAi and FaMYB10-RNAi receptacles as determined by qRT-PCR. Fruits transformed with pFRN empty vector were used as controls. Statistical significance was determined with Student's *t*-test in all assays. $*P < 0.05$; $**P < 0.01$; $***P < 0.001$. PAL, phenyl ammonia lyase; C4H, cinnamic acid 4-hydroxylase; 4CL, 4-coumaryl-CoA ligase; CHS, chalcone synthase; CHI, chalcone isomerase; F3H, flavanone 3-hydroxylase; F3′H, flavonoid-3′-hydroxylase; DFR1, dihydroflavonol reductase; CCR, (hydroxy)cinnamoyl CoA reductase; CAD, cinnamyl alcohol dehydrogenase; FLS, flavonol synthase; UF3GT, UDP:flavonol 3-glucosyltransferase; LAR, leucoanthocyanidin reductase; ANR, anthocyanidin reductase; ANS, anthocyanidin synthase; GT1, anthocyanin 3-glucosyltransferase; MT, malonyltransferase.

were downregulated in FaMYB123 and FaMYB10 transgenic fruits (Figure 5 and Figure S5b).

FaFLS, FaF3′H, and FaUF3GT, which are responsible for the synthesis of kaempferol and kaempferol-3-glucose, were also seemingly downregulated in FaMYB123 fruits but not differentially regulated in FaMYB10 fruits – by exception, FaFLS was apparently controlled by both TFs (Figure 5). Therefore, FaMYB123 is a putative regulator of anthocyanin/flavonol derivatives. We also found overexpression on the transcript level of enzymes related to proanthocyanidin biosynthesis such as FaANR and FaLAR (Figure 5) in FaMYB123 knockdown receptacles but no differences in FaMYB10 transgenic receptacles.

FaMYB123 interacts with FabHLH3 to transactivate the *FaMT1* promoter

The biosynthesis of proanthocyanidins and anthocyanins is regulated by interactions between FabHLH3 and a MYB TF (Xu et al., 2021). This led us to explore the potential interaction between the anthocyanin regulator FaMYB123 and FabHLH3 by yeast two-hybrid (Y2H) screening and bimolecular fluorescent complementation (BiFC). Yeasts transformed with FaMYB123 fused to the GAL4 DNA-binding domain and FabHLH3 fused to the GAL4 activation domain grew successfully on media supplemented with 10 mM 3-aminotriazole (3-AT) but containing no Trp, Leu, and His, indicating the two proteins interact (Figure 6a). A combination of FabHLH3 and FaMYB9, which were previously reported to interact mutually (Schaart et al., 2013), was used as a positive control. Interaction was further confirmed by bombarding epidermal onion (*Allium cepa*) cells (i.e., a BiFC assay). The two proteins were found to interact in nuclei; also, no fluorescence was detected in the negative controls (Figure 6b).

FaMYB123 and FabHLH3 TFs acted cooperatively in transactivating the 2000-bp promoter region upstream of the start codon of *FaMT1* – which is the most downregulated malonyltransferase gene in transgenic fruits – when fused to the β-glucuronidase (GUS) reporter gene in *N. benthamiana* leaves. *In silico* analysis revealed several MYB-binding boxes in the *FaMT1* promoter, which suggests that FaMYB123 might bind directly to it and transactivate *FaMT1* expression as a result (Figure S6). FaMYB123 substantially transactivated the *FaMT1* promoter by itself, but its activity was further increased by coinfiltration with FabHLH3 (Figure 7). On the other hand, FabHLH3 in isolation exhibited no transactivation activity. This result confirmed the previously noted interaction between FaMYB123 and FabHLH3. Infiltrating FaMYB10, either alone or together with FabHLH3, caused no transactivation (Figure 7). Therefore, *FaMT1* gene expression in the flavonoid/phenylpropanoid biosynthetic pathway is directly governed by FaMYB123.

DISCUSSION

A number of metabolic pathways involved in the fruit ripening process are behind the many physiological quality-related processes that confer strawberry some of its sensory properties, including color, aroma, and flavor. These

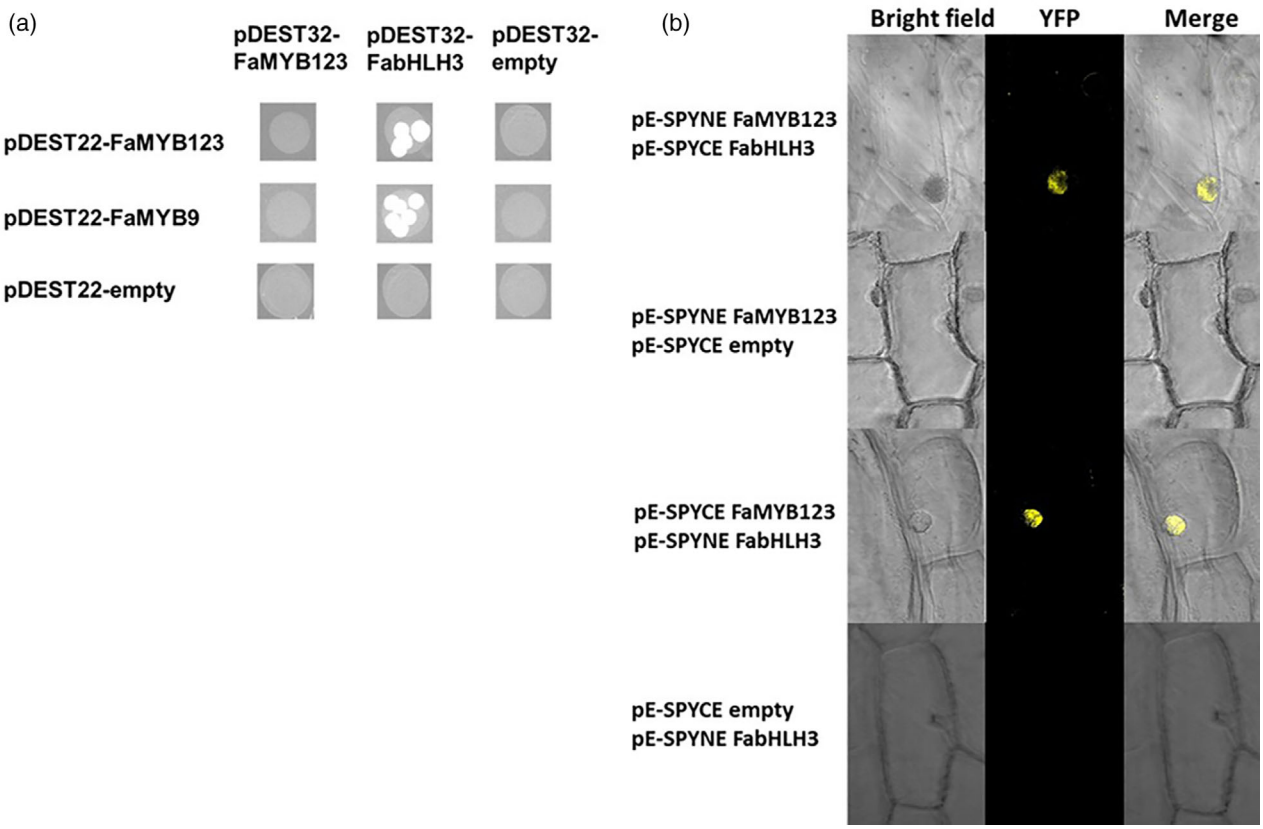

Figure 6. (a) Yeast two-hybrid assay for the interaction between FaMYB123 and FabHLH3. ORFs of the TFs FaMYB123, FabHLH3, and FaMYB9 were recombined into the bait vector (pDEST32) and prey vector (pDEST22). The yeast stains used in the drop test were PJ69-4a (MATa) and PG69-4α (MATα). pDEST32-FabHLH3 and pDEST22-FaMYB9 were used as positive controls. The empty vectors pDEST22 or pDEST32 were also cotransformed as negative controls. The ability of yeast cells to grow on synthetic defined medium lacking Leu, Trp, and His but containing 10 mM 3-AT was scored as a positive interaction. (b) BiFC. Reconstruction of YFP in the nuclei of bombarded onion (*Allium cepa*) epidermal cells transformed with constructs harboring genes encoding FaMYB123 and FabHLH3 fused with YFP halves. Merge indicates digital merging of brightfield and fluorescent images.

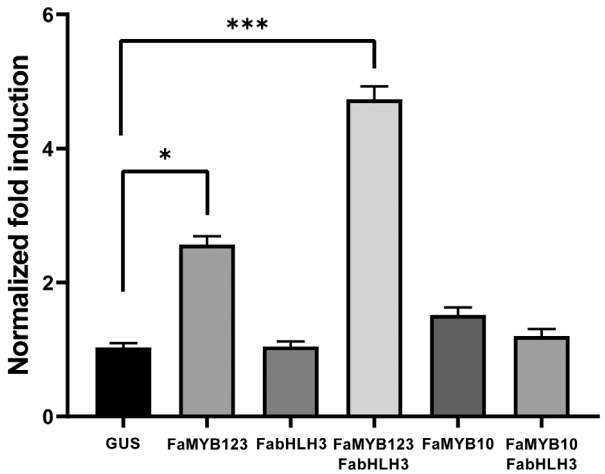

Figure 7. Synergistic transactivation of the *FaMT1* promoter by MYB123 and bHLH3 in *N. benthamiana*. Quantitative measurement of GUS enzyme activity in tobacco leaves transiently expressing the *FaMT1* promoter construct (pFaMT1:eGFP-GUS) and FaMYB123, FabHLH3, and FaMYB10 ORFs as effectors driven by the CaMV 35S promoter. The *y*-axis shows the fold change values of GUS activity relative to control transfected with pCaMV35S:eGFP-GUS. The results represent three independent experiments (n = 6–8 biological repeats) and error bars represent the SEM. Statistical significance was determined with Student's *t*-test.

molecular pathways are finely regulated by various TFs (Aharoni et al., 2001; Daminato et al., 2013; Medina-Puche et al., 2014; Medina-Puche et al., 2015; Molina-Hidalgo et al., 2017; Vallarino et al., 2020; Zhang et al., 2018). Based on our results, the interaction between FaMYB123 and FabHLH3 boosts anthocyanin/flavonoid production at the ripening stages. In this study, a new function for an R2R3 MYB TF has been elucidated, regulating a malonyltransferase involved in the biosynthesis of cyanidin and pelargonidin malonyl derivatives.

FaMYB123, a MYB-like TF, is ripening-related and hormonally regulated

Based on bioinformatic analysis, the deduced FaMYB123 protein, like other MYB TFs, contains the typical R2R3 MYB domains (Figure S1b) (Lipsick, 1996). Sequencing analysis showed that it was shorter than the predicted sequence in the Genome Database for Rosaceae (Figure S1a). Therefore, the prediction for this gene was wrong, and so were those for other MYB TFs in strawberry (Xu et al., 2021) and for NAC TFs (Moyano et al., 2018). A phylogenetic analysis with protein sequences of MYB TFs with inferred function revealed that FaMYB123 is very similar to transparent testa MYB TFs such as *A. thaliana* AtTT2, *Vitis vinifera* VvMYBPA2, and *Actinidia chinensis* AcMYB123 (Figure 1). TT2 TFs, including AtTT2 and VvMYBPA2, have been associated with the regulation of structural genes linked to proanthocyanidin production (Baudry et al., 2004; Terrier et al., 2009). However, other TT2-like TFs, such as AcMYB123 and MdMYB9, were recently deemed regulators of the production of anthocyanins in fruits (Wang et al., 2018; Wang et al., 2019).

Most of the genes that encode enzymes influencing the sensory properties of strawberry receptacles share a common overall gene expression model. Such genes are induced throughout receptacle ripening, exhibit receptacle-specific expression, and have their expression activated by ABA but repressed by auxins (Medina-Puche et al., 2016). The expression profiles of functionally characterized TFs involved in the ripening process such as FaMYB10 (Medina-Puche et al., 2014), FaEOBII (Medina-Puche et al., 2015), FaDOF2 (Molina-Hidalgo et al., 2017), and FaSCR (Pillet et al., 2015) are identical with that of FaMYB123. Interestingly, these TFs regulate expression of structural genes belonging to discrete nodes of the flavonoid biosynthetic pathway and are responsible for some fruit quality characteristics. *FaMYB123* was largely expressed at the late stages of ripening (R, OR) but found at low levels at early development stages (Figure 2a). Likewise, *FaMYB123* was expressed mainly in receptacles, but not in achenes at any stage (Figure 2c); also, it was weakly expressed in vegetative tissues (Figure 2b). The parallel expression pattern of these TFs, together with the phylogenetic relationship with the TT2-like TFs, suggests that FaMYB123 may regulate genes involved in the flavonoid biosynthetic pathway.

FaMYB123, together with FaMYB10, regulates the anthocyanin pathway in strawberry

The metabolomic changes observed in FaMYB123-RNAi transgenic receptacles revealed a substantial reduction in total anthocyanin content and an increase in proanthocyanidin content (Figure 4a–c, Table S1). In strawberry fruits, anthocyanins are synthetized during ripening and proanthocyanidins at early growth and development stages (Aaby et al., 2007; Buendia et al., 2010). We found a marked decrease in anthocyanins of strawberry fruits, including pelargonidin-3-glucose, cyanidin-3-glucose, and their malonyl derivatives pelargonidin 3-(6″-malonylglucoside) and cyanidin 3-(6″-malonylglucoside) (Figure 4c). These results are consistent with the observed downregulation of *FaANS* and *FaGT1* in FaMYB123-RNAi receptacles (Figure S7). Both are structural genes encoding the last enzymes in the anthocyanin metabolic pathway, which catalyze the synthesis of pelargonidin and pelargonidin-3-glucoside, respectively (Almeida et al., 2007; Griesser et al., 2008). Indeed, FaGT1 knockdown markedly reduced the contents of pelargonidin-3-glucose and its malonyl derivative (Griesser et al., 2008).

Quantitative trait locus (QTL) studies comparing different hybrid populations of woodland strawberry (*Fragaria vesca*) have revealed a QTL associated with the presence or absence of pelargonidin 3-(6″-malonylglucoside) and seven genes encoding putative phenolic glucoside malonyltransferases (Davik et al., 2020). Two of the genes (*FaMT1* and *FaMT5*) were upregulated in ripe

Fragaria × *ananassa* fruits (Figure S5a). However, their expression in FaMYB123-RNAi receptacles was downregulated (Figure S5b), which suggests that this TF might control the biosynthesis of pelargonidin 3-(6″-malonylglucoside) by regulating the above malonyltransferases in strawberry ripe receptacles.

A marked reduction in metabolites of the flavonol pathway was observed concomitantly with the reduction in *FaUF3GT* transcript level (Figure S7). This gene bears high sequence homology with a flavonoid 3-glucosyltransferase from *Rosa hybrida* (*RhUF3GT*), which is responsible for the synthesis of kaempferol-3-glucoside (Fukuchi-Mizutani et al., 2011). Flavonols such as kaempferol-3-glucoside and kaempferol 3-(6″-malonylglucoside) and compounds such as quercitin-3-glucoside and quercitin-3-(6″-malonylglucoside) were found at decreased levels in transgenic receptacles (Figure S7). These results suggest that FaMYB123 directly or indirectly controls not only the late steps of the anthocyanin pathway but also other branches of the flavonoid metabolic pathway related to the biosynthesis of flavonol compounds such as kaempferol and quercetin (Figure S7). *FaMYB123* knockdown resulted in increased expression of *FaANR* and *FaLAR*, which encode an anthocyanidin reductase and a leucoanthocyanidin reductase, respectively. Both enzymes are involved in the synthesis of epicatechin, epiafzelechin and related compounds (Figure S7). These upregulating effects on gene expression are in line with the increased levels of flavan-3-ols such as catechin and epicatechin, their monohydroxylated equivalents afzlechin and epiafzlechin, and their glycosylated derivatives.

Our comparative expression analysis between transgenic receptacles of FaMYB10-RNAi and FaMYB123-RNAi revealed that the biosynthetic genes involved in the early steps of the anthocyanin pathway (viz., *FaPAL*, *FaCHS*, and *FaCHI*) were regulated mainly by FaMYB10 but unaffected by the downregulation of *FaMYB123*. On the other hand, the genes involved in the late steps (viz., *FaANS*, *FaGT1*, and *FaMT1*) appeared to be regulated by both TFs. Also, the genes involved in branches leading to the production of flavonols (*FaF'3H* and *FaUF3GT*) and proanthocyanidins (*FaANR* and *FaLAR*) were upregulated in FaMYB123-RNAi receptacles, possibly as a result of the metabolic flux being redirected in response to the absence of late biosynthetic enzymes. A possible role for FaMYB123 as a negative regulator of the proanthocyanidin branch must be explored in the future, in a similar way that has been proposed for MrMYB6, which by interacting with MrbHLH1 and MrWD40-1 directly represses the promoter activities of the proanthocyanidin-specific genes *MrLAR* and *MrANR* in Chinese bayberry (*Morella rubra*) (Shi et al., 2021). However, those enzymes were not affected by *FaMYB10* downregulation. The changes found in phenylpropanoid metabolism in FaMYB123-RNAi receptacles were similar to those in FaMYB10-RNAi, where a marked decrease in pelargonidin-3-glucoside, pelargonidin 3-(6″-malonylglucoside), cyanidin-3-glucoside, kaempferol-3-glucose, kaempferol-3-glucuronide, and quercitin-3-glucuronide was observed (Medina-Puche et al., 2014). However, the increased expression of *FaANR* and *FaLAR* led to FaMYB123-RNAi fruits having increased contents of proanthocyanins. These results suggest that FaMYB10 and FaMYB123 may regulate different sets of genes encoding enzymes involved in this metabolic pathway. A similar coregulation pattern was previously reported for bilberry (*Vaccinium myrtillus* L.) with TFs MYBPA1 and MYBPA2 contributing to anthocyanin biosynthesis during berry ripening by directly activating key biosynthetic genes (Karppinen et al., 2021). During ripening, VmMYBPA2.2, together with VmMYBA1 and VmMYBPA1.1, boosts production of anthocyanins in the delphinidin branch. VmMYBPA2.2 was previously shown to activate the promoters of *DFR*, *ANS*, and, especially, *F3′5′H*.

FaMYB123 and FabHLH3 synergistically transactivate *FaMT1* expression

A model for the regulation of proanthocyanidin synthesis in strawberry green fruits by which interactions between FaMYB9 and FabHLH3 TFs might activate *FaANR* and *FaLAR* expression (Schaart et al., 2013) was tested here by using a heterologous system where coexpression of the two TFs enabled transactivation of the *AtANR* promoter (Schaart et al., 2013). Recently, new MBW complexes including FvbHLH3, FvbHLH33, and FvMYC1 were reported to govern the synthesis and accumulation of anthocyanins in woodland strawberry (Xu et al., 2021). We propose that FabHLH3, which is constitutively expressed throughout the development and ripening stages, may play a pivotal role among the biosynthetic pathways for proanthocyanidins and flavonols/anthocyanins. Such a role relies on the MYB TF interacting with FabHLH3. Through interaction with FaMYB9, FabHLH3 activates proanthocyanidin biosynthesis in green immature fruits. Similarly, through interaction with FaMYB123, it might activate expression of some structural genes involved in the flavonoid/anthocyanin pathway in ripe fruits. Indeed, we obtained Y2H- and BiFC-based evidence of this physical interaction (Figure 6). In this work, we have proposed that FaMYB123 is a regulator that controls the expression of *FaMT* genes. This led us to analyze the sequence of the *FaMT1* promoter because this gene was ripening-induced and the most downregulated malonyltransferase gene upon FaMYB123 knockdown in transgenic fruits. The assay revealed the presence of several MYB recognition boxes (Figure S6). A synergistic transactivating effect of FaMYB123 and FabHLH3 on the *FaMT1* promoter was demonstrated by infiltrating *N. benthamiana* leaves (Figure 7). Based on these results, FaMYB123 might be a regulator jointly with FabHLH3.

However, FaMYB10, either alone or together with FabHLH3, was unable to transactivate the *FaMT1* promoter, even though the latter was downregulated in FaMYB10-RNAi fruits, which is suggestive of indirect regulation, although we do not discard the possibility of a missing coregulator, another bHLH that would be needed for the transactivation activity on this promoter. A complex formed by AcMYB123 and AcbHLH42 was previously found to regulate anthocyanin production in kiwifruit (*A. chinensis*) (Wang et al., 2019). AcMYB123 is a putative ortholog of FaMYB123 and, like FaMYB123, it activates expression of structural genes involved in the late steps of the flavonoid biosynthetic pathway such as *AcANS* and *AcUFGT*. Wang et al. (2019) concluded that both TFs are involved in the spatial and temporal regulation of anthocyanin biosynthesis in ripe kiwifruit. Similar results were found in apple (*Malus domestica*), where the TT2-like TF MdMYB9 and MdMYB11, recruiting MdbHLH3, regulate anthocyanin biosynthesis at low temperatures by transactivating the *MdANS* and *MdUFGT* promoters – and hence expression of the genes (Wang et al., 2018).

In summary, in this work we obtained functional data demonstrating that FaMYB123 is a ripening-related, receptacle-specific TF. *FaMYB123* is strongly regulated by both ABA and auxins, the key hormones governing fruit ripening. Based on gene expression and metabolomic data for transgenic receptacles, FaMYB123 specifically regulates the late steps of the flavonoid pathway, that is, the production of pelargonidin-3-glucose, cyanidin-3-glucose, and their malonyl derivatives pelargonidin 3-(6″-malonylglucoside) and cyanidin 3-(6‴-malonylglucoside) – which are the most abundant anthocyanins in ripe strawberry receptacles and key contributors to strawberry color – as well as flavonols such as kaempferol-3-glucoside, kaempferol 3-(6″-malonylglucoside), quercitin-3-glucoside, and quercitin-3-(6″-malonylglucoside). FaMYB123 interacts with FabHLH3, another flavonoid-related TF, to jointly regulate expression of the malonyltransferase gene *FaMT1* during ripening of strawberry fruit. FaMYB10 and FaMYB123 together may regulate different sets of genes encoding the enzymes involved in this metabolic pathway, which testifies to the high complexity of combinatory control of anthocyanin biosynthesis. Further work will be required to complete this puzzle in strawberry fruits.

EXPERIMENTAL PROCEDURES

Plant material and transgenic generation

The *Fragaria* × *ananassa* Duch. cv. Camarosa samples used were grown on El Cebollar experimental farm (Moguer, Huelva). The samples spanned fruits at six different development and ripening stages, namely, small-sized green (G1, 2–3 g), full-sized green (G3, 5–8 g), white (W, 8–12 g), full-ripe red (R, 9–15 g), overripe (OR, 9–15 g), and senescent fruits (SN, 9–15 g), and also expanding leaves, flowers, runners, and petals. All were frozen in liquid nitrogen immediately upon harvesting. The *N. benthamiana* plants used for agroinfiltration were grown in a plant chamber at 25°C, 10 000 lux, and 80% humidity and stored in a greenhouse.

For strawberry transformation, conserved regions from *FaMYB123* and *FaMYB10* were amplified by PCR for cloning first into the pCR8/GW/TOPO vector and then into the Gateway pFRN vector. Prior to transformation, the generated constructs pFRN-FaMYB123 and pFRN-FaMYB10 were sequenced. Transgenic plants were generated according to (Barcelo et al., 1998). Briefly, leaf discs of strawberry plants of cv. Chandler were transformed with *Agrobacterium tumefaciens* strain AGL1 containing pFRN-FaMYB123, pFRN-MYB10, or pFRN-empty. Explants were kept in Murashige–Skoog medium supplemented with 25 mg kanamycin L^{-1}. After 7–8 months of antibiotic selection, kanamycin-resistant regenerated shoots were screened by PCR for the presence of transgenes by amplification of the *nptII* gene. Positive clones were acclimated and transferred to a greenhouse. Silencing was assessed by comparing the *FaMYB123* and *FaMYB10* transcript levels in pFRN-FaMYB123 and pFRN-FaMYB10 red fruits with those in empty pFRN fruits. Fruit quality parameters were evaluated in FaMYB123-RNAi lines, in fruits of uniform size, with standard shape, weighing >5 g. Fruit color was measured with a colorimeter (Minolta Chroma Meter CR-400, Osaka, Japan). The L*a*b* color space parameters (lightness, redness, yellowness) were recorded. Soluble solids were measured using a refractometer (Atago N1), and firmness was measured using a hand-held penetrometer (Effegi) with a cylindrical needle with a surface of 9.62 mm^2. A minimum of 10 ripe fruits per line were evaluated (Figure S8).

Hormone treatments

The ABA content of strawberries was reduced in two different ways. Because FaNCED1 is a key enzyme in ABA biosynthesis, we altered its function by inhibiting its expression or its enzymatic activity. *FaNCED1* expression in green fruits was reduced by agroinfiltration with a pFRN-FaNCED1 construct and its enzymatic activity was inhibited with NDGA, using up to 30–40 white fruits from 15–25 plants for this purpose. ABA is known to accumulate under water deprivation conditions. We thus used such conditions to increase its content. Up to 50 white fruits and their pedicels were harvested for this purpose. For stress treatment, fruits were kept with their pedicels outdoors, whereas control fruits were submerged in Murashige–Skoog medium. The samples thus treated were used for ABA measurement and expression analysis of FaNCED1 and FaMYB123. The ABA extraction procedure and HPLC-MS conditions are described elsewhere (Medina-Puche et al., 2014).

The content of auxin in strawberry fruits was modulated by removing its source (achenes) from two pools of 50 G3 fruits. The fruits were covered with lanolin paste to prevent dehydration and one set was treated with 1 mM IAA to assess the relative expression levels of FaMYB123.

Bioinformatic tools

Bioinformatic analyses were conducted with resources of the European Bioinformatics Institute server (InterPro, ClustalW2) and the National Center for Biotechnology Information (BlastP, BlastX). Subcellular localization was performed with CELLO2Go. Strawberry sequences were obtained from the GDR database, using the last available *F. vesca* genome (v. 4.01) (Edger et al., 2019). The *FaMT1* promoter was analyzed using the PlantCARE database. The sequences for FaMYB123 alignments were downloaded from GeneBank and the TAIR database. The phylogenetic tree was constructed with FigTree using a bootstrap of 1000 replicates.

Expression analysis by quantitative real-time PCR

A minimum of three independent pools of each type of tissue were used to extract and purify total RNA as described elsewhere (Molina-Hidalgo et al., 2015). cDNA was obtained with an iScript kit from Bio-Rad and used in the qRT-PCR reaction in an iCycler system also from Bio-Rad. Relative differential expression was determined by using the $2^{-\Delta\Delta Ct}$ method (Pedersen & Amtssygehus, 2001). The interspacer 26S–18S, which exhibits constitutive expression under all tested experimental conditions (Amil-Ruiz et al., 2013), was used as an internal reference. Every reaction was performed at least in triplicate, the presence of a single amplicon being inferred from melting temperatures. The primers used are listed in Table S2.

Total anthocyanin analysis

Approximately 100 mg of frozen tissue from fruit receptacles was poured into 1 ml of 1% (v/v) hydrochloric acid/methanol mixture and kept at 4°C under continuous stirring for 10 min. The resulting slurry was centrifuged at 1500 ***g*** at 4°C for 10 min and the anthocyanin content was determined by measuring the absorbance at 515 nm using the following formula: E_{molar} = 36 000 L mol^{-1} cm^{-1} (Bustamante et al., 2009; Woodward, 1972). Each analysis was replicated six times.

Metabolite extraction, HPLC analysis, and identification

For LC-MS analysis, approximately 100 mg of frozen tissue was lyophilized in a Christ RVC 2-18 freeze-dryer for 24 h. A total of eight biological replicates were included. Lyophilized powder was added to 800 μl of pure methanol containing 0.2 μg ml^{-1} isovitexin as internal standard and incubated at 70°C for 15 min for extraction. Then, 400 μl of water was added and the mixture was centrifuged at 12 000 ***g*** for 10 min. A 400-μl aliquot was subsequently dried under vacuum for suspension in a 50% (v/v) methanol:water mixture.

Secondary metabolites were profiled on a Waters Acquity UPLC system coupled to a Q-Exactive Orbitrap mass detector as described elsewhere (Giavalisco et al., 2009). The UPLC system was equipped with an HSS T3 C18 reversed phase column (100 × 2.1 mm i.d., 1.8 μm particle size) from Waters that was operated at 40°C. The mobile phase consisted of 0.1% formic acid in water (solvent A) or acetonitrile (solvent B). The flow rate was 400 μl min^{-1}, and the injected volume was 2 μl. The UPLC system was connected to an Exactive Orbitrap from Thermo Fisher Scientific via a heated electrospray source. Spectra were recorded in full scan mode with negative and positive ion detection in a mass range of *m*/*z* 100 to 1500 and were recorded from minute 0 to 19 of the UPLC gradient. Molecular masses, retention times, and associated peak intensities were extracted from raw files by using RefinerMS v. 5.3 from GeneData and Xcalibur (Thermo Fisher Scientific, Waltham, MA USA). Metabolites were identified and annotated against standards and extracted from (Del Bubba et al., 2012; D'Urso et al., 2016; Enomoto et al., 2018; Vallarino et al., 2020). Data are reported in a format compliant with the standards proposed by (Fernie et al., 2011). A comprehensive list of the metabolites identified is provided in Table S1.

Cloning of the full-length sequence of *FaMYB123* and subcellular localization of the coded protein

For subcellular localization, the full-length FaMYB123 coding sequence (CDS) was amplified by PCR with specific primers and transferred to the pDONR221 vector by using the BP recombination reaction (Invitrogen, Waltham, MA USA). Subsequently, LR recombination was used to transfer the full-length CDS to the pK7WGF2.0 vector, which enabled N-terminal fusion of GFP to the target protein and produced 35S-GFP-FaMYB123. The resulting construct was sequenced prior to transforming *Nicotiana* leaves according to (Molina-Hidalgo et al., 2015).

Yeast two-hybrid assay

Protein–protein interactions were examined by Y2H using the LR reaction to transfer the FaMYB123 CDS from pDONR221 to the pBDGAL4 bait vector (pDEST32; Invitrogen) and the pADGAL4 prey vector (pDEST22; Invitrogen). The yeast strains PJ69-4α (MATα) and PJ69-4a (MATa) were used (James et al., 1996). Y2H was performed according to (de Folter et al., 2005). Briefly, for each interaction examined, 5 μl of liquid culture was plated on yeast medium lacking His, Leu, and Trp supplemented with 10 mM 3-AT. Plates were incubated at 28°C for 3 days, using pDEST32-FabHLH3 and pDEST22-FaMYB9, which were kindly supplied by Dr. Jan Schaart (Wageningen UR Plant Breeding, the Netherlands), as positive controls. The GenBank accession numbers for the genes are: FaMYB9, JQ989281; FabHLH3, JQ989284.

BiFC assays were performed by fusing the FaMYB123 and FabHLH3 full-length CDSs to the N- and C-terminal domains of yellow fluorescent protein (YFP) (pE-SPYNE-GW and pE-SPYCE-GW, respectively, which were kindly supplied by Drs. Caroline Mayer and Wolfgang Dröge-Laser of Lehrstuhl für Pharmazeutische Biologie, Julius-Maximilians Universität Würzburg), through the LR reaction. Fresh epidermal onion peels were co-bombarded with 1-μm gold particles coated with appropriate DNA constructs using a DuPont PDS-1000 biolistic helium gun device from Bio-Rad. Fluorescence emission was measured with an Axio Observer.Z1 motorized inverted microscope after 48 h of incubation at 22°C in the dark.

Agrobacterium-mediated transient expression and fluorimetric assay of GUS activity

The genome sequence of *Fragaria* × *ananassa* was obtained from GDR and the 2000-bp region upstream of the predicted start codon (the putative promoter region of *FaMT1*) (FvH4_6g46741) was examined. The synthetized fragment was cloned into the binary vector pKGWFS7, fusing the promoter to the eGFP and GUS CDSs. Positive vectors were transformed into *A. tumefaciens* strain GV3101 and selected by using suitable antibiotics.

Transient expression in *N. benthamiana* leaves was assessed according to (Schutze et al., 2009). Briefly, an overnight *Agrobacterium* culture was resuspended in AS medium (10 mM $MgCl_2$, 10 mM morpholine ethanesulfonic acid [MES] [pH 5.6], and 150 μM acetosyringone) and incubated at room temperature for 2 h. Leaves from 4-week-old *N. benthamiana* plants were transfected with a pFaMT1:eGFP-GUS reporter construct and effector constructs overexpressing GUS, MYB123, bHLH3, MYB10, or a combination thereof and collected 3 days after infiltration. Uninfiltrated leaves and the pKGWFS7 empty vector were used as negative controls, and pCaMV35S:eGFP-GUS was used as a positive control. The number of infiltrated leaves ranged from four to six per construct. All construct combinations were coinfiltrated with the pBln61-p19 construct.

GUS concentrations were determined by grinding infiltrated leaf discs in liquid nitrogen and extracting protein with modified CCRL buffer (100 mM K-phosphate [pH 7.8], 1 mM EDTA, 10% glycerol) to which 7 mM β-mercaptoethanol, 0.1% Triton X-100 (Luehrsen et al., 1992), and 2% polyvinylpolypyrrolidone (PVPP) were added before use. The homogenate was centrifuged and the clear supernatant was used to quantify either protein content (Bradford, 1976) or reporter activity. The GUS assay involved incubating

10 μl of extract added to 100 μl of 1 mM 4-methylumbelliferyl-β-glucuronide. 4-Methylumbelliferone thus released was quantified with a Varioskan™ Lux microplate reader from ThermoFisher Scientific. All GUS activity values were normalized to total protein content, and the numerical values from the GUS activity fluorimetric assay for all samples were normalized to the pCaMV35S:eGFP-GUS positive control. Statistical significance was assessed with unpaired Student's *t*-tests.

Statistical analysis

Statistical significance was checked with one-way analysis of variance (ANOVA) and Scheffe's post-hoc test or Student's *t*-test as implemented in SPSS software.

AUTHOR CONTRIBUTIONS

FMR and FJMH performed the experiments, analyzed the data, and wrote the manuscript. PRV and JAM generated the transgenic plants. LMP, VGS, JLC, and RBP provided technical assistance to FMR and FJMH. LMC, MS, ARF, and SA helped with LC-MS and metabolic analyses. JMB conceived and codirected the project with FJMH and helped to write the manuscript with valuable suggestions from all other authors.

ACKNOWLEDGMENTS

This work was funded by the Spanish Ministerio de Ciencia e Innovación (AGL2014-55784-C2-2-R and AGL2017-86531-C2-2-R). FJMR is supported by a 'Margarita Salas' post-doctoral fellowship (UCOR02MS) from the University of Córdoba (Requalification of the Spanish university system) from the Ministry of Universities financed by the European Union (NexGenerationEU). FJMH is supported by a 'Juan de la Cierva-Incorporación' fellowship (IJC2020-045526-I), funded by MCIN/AEI/10.13039/501100011033 and the European Union 'NextGenerationEU'/PRTR. AR-F and SA are on the European Union's Horizon 2020 Research and Innovation Program, Project PlantaSYST (SGA-CSA No. 739582 under FPA No. 664620). The authors thank Dr. Gema García from the Microscopy Unit of UCAIB-IMIBIC for technical help with the microscope. Funding for open access charge: University of Cordoba/CBUA.

CONFLICT OF INTEREST

The authors declare no competing interests.

DATA AVAILABILITY STATEMENT

The authors confirm that all data referred to here are available in the body of this article and its supplementary materials.

SUPPORTING INFORMATION

Additional Supporting Information may be found in the online version of this article.

Figure S1. (a) *FaMYB123* sequence obtained by PCR with cDNA from red fruits (*Fragaria* × *ananassa* Duch. cv. Camarosa) as compared with the putative sequence of the predicted ortholog *FvH4_5g32460* from *Fragaria vesca* (Genome v4.0.a2). (b) Predicted domains of FaMYB123 protein as identified with InterPro. (c) Subcellular location of FaMYB123 protein as predicted on the CELLO2Go website.

Figure S2. Phylogenetic tree of MYB transcription factors from *Arabidopsis thaliana* (sequences downloaded from the TAIR database) with all *Fragaria* × *ananassa* proteins (downloaded from the plantTFDB database).

Figure S3 (a) Partial protein sequence alignment of FaMYB123 and its homologs from higher plant species. R2 and R3 repeat domains and the conserved bHLH interaction motif (D/E)LX_2(R-K)$X_3LX_6LX_3R$ are outlined with a black box and marked with asterisks. (b) Protein sequence alignment of FabHLH3 and homologs from other plant species. The three conserved motifs of the N-terminal MYB interaction region are indicated with boxes 11, 18, and 13, and the C-terminal basic helix1–loop–helix2 domain is outlined with a black box.

Figure S4. qRT-PCR analysis of *FaMYB123* and *FaMYB10* gene expression in transgenic FaMYB123-RNAi strawberry fruits (*Fragaria* × *ananassa* cv. Elsanta) transformed with the empty pFRN vector (control) and the pFRN-FaMYB123 construct. *FaMYB10* expression was used as an indicator of ripening stage. Statistical significance with respect to the reference sample was determined with Student's *t*-test. $^{***}P < 0.001$.

Figure S5. (a) Expression pattern of *Fragaria* × *ananassa* malonyltransferase genes in different tissues and during fruit receptacle development and ripening. The patterns were analyzed by heatmapping runners (Ru), leaves (Le), flowers (Fl), petals (Pe), and small-sized green (G1), full-sized green (G3), white (W), full-ripe red (R), overripe (OR), and senescent fruits (SE). On the color scale on the right, red represents high contents and green represents low contents. Heatmaps were constructed with GraphPad Prism v. 8.0.1. (b) qRT-PCR analysis of *FaMT1* and *FaMT5* expression in transgenic FaMYB123-RNAi strawberry fruits (*Fragaria* × *ananassa* cv. Elsanta) transformed with the empty pFRN vector (Control) and the pFRN-FaMYB123 construct (L28, L31, and L32). Statistical significance with respect to the reference sample was determined with Student's *t*-test.

Figure S6. Schematic depiction of the *FvMT1* promoter from *Fragaria vesca*. The upper bar shows the length of the promoter fragment relative to the ATG start codon. The location of the MYB motif is shown with black lines.

Figure S7. Schematic depiction of the phenylpropanoid, flavonoid, and anthocyanin pathways. Enzymes that were upregulated or downregulated by FaMYB123 knockdown based on the data from Figure 5 are shown with arrows pointing up and down, respectively. Boxplots represent the levels of metabolites in control and transgenic receptacles, the *y*-axis showing the normalized area of each compound in the LC-MS analysis. PAL, phenyl ammonia lyase; 4CL, 4-coumaryl-CoA ligase; ANS, anthocyanidin synthase; C4H, cinnamic acid 4-hydroxylase; CHI, chalcone isomerase; CHS, chalcone synthase; DFR, dihydroflavonol reductase; F3H, flavanone 3-hydroxylase; F3′H, flavonoid-3′-hydroxylase; GT1, anthocyanin 3-glucosyltransferase; MT, malonyltransferase; UF3GT, UDP: flavonol 3-glucosyltransferase. $^{**}P < 0.001$.

Figure S8. Phenotypic analysis of transgenic plants. Transgenic plants were evaluated during the growing seasons, using non-transformed plants (cv. Chandler) as control. Plants were grown in a greenhouse under natural temperature and light conditions and fruit was collected from March to July. Eight plants per line and a minimum of 10 ripe fruits per line were evaluated. Fruits were harvested at the stage of full ripeness, when the fruit surface was completely red, and the weight, size, color, soluble solids, and firmness were recorded. Color was measured using a colorimeter (Minolta Chroma Meter CR-400, Osaka, Japan). The instrument was calibrated with a standard white and a standard black reflective plate before use. The L*a*b* color space parameters

(lightness, redness, yellowness) were recorded. Soluble solids were measured using a refractometer (Atago N1), and firmness was measured using a hand penetrometer (Effegi) with a cylindrical needle with an area of 9.62 mm^2.

Table S1. Complete data from the liquid chromatography–mass spectrometry analysis as normalized against the internal standard and fresh weight. A total of eight replicates were used under each condition.

Table S2. Primer sequences used. Fw, forward; Rv, reverse; Up, upper; Low, lower.

REFERENCES

Aaby, K., Ekeberg, D. & Skrede, G. (2007) Characterization of phenolic compounds in strawberry (*Fragaria* × *ananassa*) fruits by different HPLC detectors and contribution of individual compounds to total antioxidant capacity. *Journal of Agricultural and Food Chemistry*, **55**, 4395–4406.

Aaby, K., Mazur, S., Nes, A. & Skrede, G. (2012) Phenolic compounds in strawberry (*Fragaria* × *ananassa* Duch.) fruits: composition in 27 cultivars and changes during ripening. *Food Chemistry*, **132**, 86–97.

Aaby, K., Skrede, G. & Wrolstad, R.E. (2005) Phenolic composition and antioxidant activities in flesh and achenes of strawberries (Fragaria ananassa). *Journal of Agricultural and Food Chemistry*, **53**, 4032–4040.

Aharoni, A., De Vos, C.H.R., Wein, M., Sun, Z.K., Greco, R., Kroon, A. *et al.* (2001) The strawberry FaMYB1 transcription factor suppresses anthocyanin and flavonol accumulation in transgenic tobacco. *Plant Journal*, **28**, 319–332.

Almeida, J.R., D'Amico, E., Preuss, A., Carbone, F., de Vos, C.H., Deiml, B. *et al.* (2007) Characterization of major enzymes and genes involved in flavonoid and proanthocyanidin biosynthesis during fruit development in strawberry (*Fragaria* × *ananassa*). *Archives of Biochemistry and Biophysics*, **465**, 61–71.

Amil-Ruiz, F., Garrido-Gala, J., Blanco-Portales, R., Folta, K.M., Munoz-Blanco, J. & Caballero, J.L. (2013) Identification and validation of reference genes for transcript normalization in strawberry (*Fragaria* × *ananassa*) defense responses. *PLoS One*, **8**, e70603.

An, X.H., Tian, Y., Chen, K.Q., Liu, X.J., Liu, D.D., Xie, X.B. *et al.* (2015) MdMYB9 and MdMYB11 are involved in the regulation of the JA-induced biosynthesis of anthocyanin and Proanthocyanidin in apples. *Plant and Cell Physiology*, **56**, 650–662.

Appelhagen, I., Lu, G.H., Huep, G., Schmelzer, E., Weisshaar, B. & Sagasser, M. (2011) TRANSPARENT TESTA1 interacts with R2R3-MYB factors and affects early and late steps of flavonoid biosynthesis in the endothelium of Arabidopsis thaliana seeds. *The Plant Journal*, **67**, 406–419.

Barcelo, M., El-Mansouri, I., Mercado, J.A., Quesada, M.A. & Alfaro, F.P. (1998) Regeneration and transformation via agrobacterium tumefaciens of the strawberry cultivar Chandler. *Plant Cell, Tissue and Organ Culture*, **54**, 29–36.

Baudry, A., Heim, M.A., Dubreucq, B., Caboche, M., Weisshaar, B. & Lepiniec, L. (2004) TT2, TT8, and TTG1 synergistically specify the expression of BANYULS and proanthocyanidin biosynthesis in Arabidopsis thaliana. *The Plant Journal*, **39**, 366–380.

Bemer, M., van Dijk, A.D.J., Immink, R.G.H. & Angenent, G.C. (2017) Cross-family transcription factor interactions: an additional layer of gene regulation. *Trends in Plant Science*, **22**, 66–80.

Bradford, M.M. (1976) A rapid and sensitive method for the quantitation of microgram quantities of protein utilizing the principle of protein-dye binding. *Analytical Biochemistry*, **72**, 248–254.

Buendia, B., Gil, M.I., Tudela, J.A., Gady, A.L., Medina, J.J., Soria, C. *et al.* (2010) HPLC-MS analysis of proanthocyanidin oligomers and other phenolics in 15 strawberry cultivars. *Journal of Agricultural and Food Chemistry*, **58**, 3916–3926.

Bustamante, C.A., Civello, P.M. & Martinez, G.A. (2009) Cloning of the promoter region of beta-xylosidase (FaXyl1) gene and effect of plant growth regulators on the expression of FaXyl1 in strawberry fruit. *Plant Science*, **177**, 49–56.

Daminato, M., Guzzo, F. & Casadoro, G. (2013) A SHATTERPROOF-like gene controls ripening in non-climacteric strawberries, and auxin and abscisic acid antagonistically affect its expression. *Journal of Experimental Botany*, **64**, 3775–3786.

Davik, J., Aaby, K., Buti, M., Alsheikh, M., Šurbanovski, N., Martens, S. *et al.* (2020) Major-effect candidate genes identified in cultivated strawberry (Fragaria × ananassa Duch.) for ellagic acid deoxyhexoside and pelargonidin-3-O-malonylglucoside biosynthesis, key polyphenolic compounds. *Horticulture Research*, **7**, 125.

de Folter, S., Immink, R.G.H., Kieffer, M., Parenicova, L., Henz, S.R., Weigel, D. *et al.* (2005) Comprehensive interaction map of the Arabidopsis MADS box transcription factors. *Plant Cell*, **17**, 1424–1433.

Del Bubba, M., Checchini, L., Chiuminatto, U., Doumett, S., Fibbi, D. & Giordani, E. (2012) Liquid chromatographic/electrospray ionization tandem mass spectrometric study of polyphenolic composition of four cultivars of Fragaria vesca L. berries and their comparative evaluation. *Journal of Mass Spectrometry*, **47**, 1207–1220.

D'Urso, G., Maldini, M., Pintore, G., d'Aquino, L., Montoro, P. & Pizza, C. (2016) Characterisation of Fragaria vesca fruit from Italy following a metabolomics approach through integrated mass spectrometry techniques. *LWT*, **74**, 387–395.

Edger, P.P., Poorten, T.J., VanBuren, R., Hardigan, M.A., Colle, M., McKain, M.R. *et al.* (2019) Origin and evolution of the octoploid strawberry genome. *Nature Genetics*, **51**, 541–547.

Enomoto, H., Sato, K., Miyamoto, K., Ohtsuka, A. & Yamane, H. (2018) Distribution analysis of anthocyanins, sugars, and organic acids in strawberry fruits using matrix-assisted laser desorption/ionization-imaging mass spectrometry. *Journal of Agricultural and Food Chemistry*, **66**, 4958–4965.

Fernie, A.R., Aharoni, A., Willmitzer, L., Stitt, M., Tohge, T., Kopka, J. *et al.* (2011) Recommendations for reporting metabolite data. *Plant Cell*, **23**, 2477–2482.

Fossen, T., Rayyan, S. & Andersen, O.M. (2004) Dimeric anthocyanins from strawberry (Fragaria ananassa) consisting of pelargonidin 3-glucoside covalently linked to four flavan-3-ols. *Phytochemistry*, **65**, 1421–1428.

Fukuchi-Mizutani, M., Akagi, M., Ishiguro, K., Katsumoto, Y., Fukui, Y., Togami, J. *et al.* (2011) Biochemical and molecular characterization of anthocyanidin/flavonol 3-glucosylation pathways in Rosa × hybrida. *Plant Biotechnology*, **28**, 239–244.

Giampieri, F., Alvarez-Suarez, J.M. & Battino, M. (2014) Strawberry and human health: effects beyond antioxidant activity. *Journal of Agricultural and Food Chemistry*, **62**, 3867–3876.

Giampieri, F., Forbes-Hernandez, T.Y., Gasparrini, M., Alvarez-Suarez, J.M., Afrin, S., Bompadre, S. *et al.* (2015) Strawberry as a health promoter: an evidence based review. *Food & Function*, **6**, 1386–1398.

Giampieri, F., Tulipani, S., Alvarez-Suarez, J.M., Quiles, J.L., Mezzetti, B. & Battino, M. (2012) The strawberry: composition, nutritional quality, and impact on human health. *Nutrition*, **28**, 9–19.

Giavalisco, P., Kohl, K., Hummel, J., Seiwert, B. & Willmitzer, L. (2009) 13C isotope-labeled metabolomes allowing for improved compound annotation and relative quantification in liquid chromatography-mass spectrometry-based metabolomic research. *Analytical Chemistry*, **81**, 6546–6551.

Griesser, M., Hoffmann, T., Bellido, M.L., Rosati, C., Fink, B., Kurtzer, R. *et al.* (2008) Redirection of flavonoid biosynthesis through the down-regulation of an anthocyanidin glucosyltransferase in ripening strawberry fruit. *Plant Physiology*, **146**, 1528–1539.

James, P., Halladay, J. & Craig, E.A. (1996) Genomic libraries and a host strain designed for highly efficient two-hybrid selection in yeast. *Genetics*, **144**, 1425–1436.

Karppinen, K., Lafferty, D.J., Albert, N.W., Mikkola, N., McGhie, T., Allan, A.C. *et al.* (2021) MYBA and MYBPA transcription factors co-regulate anthocyanin biosynthesis in blue-coloured berries. *New Phytologist*, **232**, 1350–1367.

Kranz, H., Scholz, K. & Weisshaar, B. (2000) c-MYB oncogene-like genes encoding three MYB repeats occur in all major plant lineages. *Plant Journal*, **21**, 231–235.

Kranz, H.D., Denekamp, M., Greco, R., Jin, H., Leyva, A., Meissner, R.C. *et al.* (1998) Towards functional characterisation of the members of the R2R3-MYB gene family from Arabidopsis thaliana. *Plant Journal*, **16**, 263–276.

Lai, Z.B., Schluttenhofer, C.M., Bhide, K., Shreve, J., Thimmapuram, J., Lee, S.Y. *et al.* (2014) MED18 interaction with distinct transcription factors regulates multiple plant functions. *Nature Communications*, **5**, 3064.

Lin-Wang, K., Bolitho, K., Grafton, K., Kortstee, A., Karunairetnam, S., McGhie, T.K. *et al.* (2010) An R2R3 MYB transcription factor associated with regulation of the anthocyanin biosynthetic pathway in Rosaceae. *BMC Plant Biology*, **10**, 50.

Lipsick, J.S. (1996) One billion years of Myb. *Oncogene*, **13**, 223–235.

Luehrsen, K.R., Dewet, J.R. & Walbot, V. (1992) Transient expression analysis in plants using firefly luciferase reporter gene. *Methods in Enzymology*, **216**, 397–414.

Matias-Hernandez, L., Jiang, W.M., Yang, K., Tang, K.X., Brodelius, P.E. & Pelaz, S. (2017) AaMYB1 and its orthologue AtMYB61 affect terpene metabolism and trichome development in Artemisia annua and Arabidopsis thaliana. *Plant Journal*, **90**, 520–534.

Medina-Puche, L., Blanco-Portales, R., Molina-Hidalgo, F.J., Cumplido-Laso, G., Garcia-Caparros, N., Moyano-Canete, E. *et al.* (2016) Extensive transcriptomic studies on the roles played by abscisic acid and auxins in the development and ripening of strawberry fruits. *Functional & Integrative Genomics*, **16**, 671–692.

Medina-Puche, L., Cumplido-Laso, G., Amil-Ruiz, F., Hoffmann, T., Ring, L., Rodriguez-Franco, A. *et al.* (2014) MYB10 plays a major role in the regulation of flavonoid/phenylpropanoid metabolism during ripening of *Fragaria* × *ananassa* fruits. *Journal of Experimental Botany*, **65**, 401–417.

Medina-Puche, L., Molina-Hidalgo, F.J., Boersma, M., Schuurink, R.C., Lopez-Vidriero, I., Solano, R. *et al.* (2015) An R2R3-MYB transcription factor regulates eugenol production in ripe strawberry fruit receptacles. *Plant Physiology*, **168**, 598–614.

Molina-Hidalgo, F.J., Medina-Puche, L., Canete-Gomez, C., Franco-Zorrilla, J.M., Lopez-Vidriero, I., Solano, R. *et al.* (2017) The fruit-specific transcription factor FaDOF2 regulates the production of eugenol in ripe fruit receptacles. *Journal of Experimental Botany*, **68**, 4529–4543.

Molina-Hidalgo, F.J., Medina-Puche, L., Gelis, S., Ramos, J., Sabir, F., Sovernal, G. *et al.* (2015) Functional characterization of FaNIP1;1 gene, a ripening-related and receptacle-specific aquaporin in strawberry fruit. *Plant Science*, **238**, 198–211.

Moyano, E., Martinez-Rivas, F.J., Blanco-Portales, R., Molina-Hidalgo, F.J., Ric-Varas, P., Matas-Arroyo, A.J. *et al.* (2018) Genome-wide analysis of the NAC transcription factor family and their expression during the development and ripening of the *Fragaria* × *ananassa* fruits. *PLoS One*, **13**, e0196953.

Pedersen, S. & Amtssygehus, A. (2001) Multiplex relative gene expression analysis by real-time RT-PCR using the iCycler iQ detection system. *BioRadiations*, **107**, 10–11.

Pillet, J., Yu, H.W., Chambers, A.H., Whitaker, V.M. & Folta, K.M. (2015) Identification of candidate flavonoid pathway genes using transcriptome correlation network analysis in ripe strawberry (*Fragaria* × *ananassa*) fruits. *Journal of Experimental Botany*, **66**, 4455–4467.

Schaart, J.G., Dubos, C., Romero De La Fuente, I., van Houwelingen, A., de Vos, R.C.H., Jonker, H.H. *et al.* (2013) Identification and characterization of MYB-bHLH-WD40 regulatory complexes controlling proanthocyanidin biosynthesis in strawberry (*Fragaria* × *ananassa*) fruits. *The New Phytologist*, **197**, 454–467.

Schutze, K., Harter, K. & Chaban, C. (2009) Bimolecular fluorescence complementation (BiFC) to study protein-protein interactions in living plant cells. *Methods in Molecular Biology*, **479**, 189–202.

Shi, L., Chen, X., Wang, K., Yang, M., Chen, W., Yang, Z. *et al.* (2021) MrMYB6 from Chinese bayberry (Myrica rubra) negatively regulates anthocyanin and Proanthocyanidin accumulation. *Frontiers in Plant Science*, **12**, 685654.

Terrier, N., Torregrosa, L., Ageorges, A., Vialet, S., Verries, C., Cheynier, V. *et al.* (2009) Ectopic expression of VvMybPA2 promotes proanthocyanidin biosynthesis in grapevine and suggests additional targets in the pathway. *Plant Physiology*, **149**, 1028–1041.

Vallarino, J.G., Merchante, C., Sanchez-Sevilla, J.F., de Luis Balaguer, M.A., Pott, D.M., Ariza, M.T. *et al.* (2020) Characterizing the involvement of FaMADS9 in the regulation of strawberry fruit receptacle development. *Plant Biotechnology Journal*, **18**, 929–943.

Wang, H., Cao, G.H. & Prior, R.L. (1996) Total antioxidant capacity of fruits. *Journal of Agricultural and Food Chemistry*, **44**, 701–705.

Wang, L., Tang, W., Hu, Y., Zhang, Y., Sun, J., Guo, X. *et al.* (2019) A MYB/bHLH complex regulates tissue-specific anthocyanin biosynthesis in the inner pericarp of red-centered kiwifruit Actinidia chinensis cv. Hongyang. *The Plant Journal*, **99**, 359–378.

Wang, N., Qu, C., Jiang, S., Chen, Z., Xu, H., Fang, H. *et al.* (2018) The proanthocyanidin-specific transcription factor MdMYBPA1 initiates anthocyanin synthesis under low-temperature conditions in red-fleshed apples. *The Plant Journal*, **96**, 39–55.

Wang, S.Y. & Zheng, W. (2001) Effect of plant growth temperature on antioxidant capacity in strawberry. *Journal of Agricultural and Food Chemistry*, **49**, 4977–4982.

Wang, S.Y., Zheng, W. & Galletta, G.J. (2002) Cultural system affects fruit quality and antioxidant capacity in strawberries. *Journal of Agricultural and Food Chemistry*, **50**, 6534–6542.

Woodward, J.R. (1972) Physical and chemical changes in developing strawberry fruits. *Journal of Science and Food Agriculture*, **23**, 465–473.

Wu, X. & Prior, R.L. (2005) Systematic identification and characterization of anthocyanins by HPLC-ESI-MS/MS in common foods in the United States: fruits and berries. *Journal of Agricultural and Food Chemistry*, **53**, 2589–2599.

Xie, Y., Tan, H.J., Ma, Z.X. & Huang, J.R. (2016) DELLA proteins promote anthocyanin biosynthesis via sequestering MYBL2 and JAZ suppressors of the MYB/bHLH/WD40 complex in Arabidopsis thaliana. *Molecular Plant*, **9**, 711–721.

Xu, P., Wu, L., Cao, M., Ma, C., Xiao, K., Li, Y. *et al.* (2021) Identification of MBW complex components implicated in the biosynthesis of flavonoids in woodland strawberry. *Frontiers in Plant Science*, **12**, 774943.

Xu, W.J., Dubos, C. & Lepiniec, L. (2015) Transcriptional control of flavonoid biosynthesis by MYB-bHLH-WDR complexes. *Trends in Plant Science*, **20**, 176–185.

Zhang, Y., Yin, X., Xiao, Y., Zhang, Z., Li, S., Liu, X. *et al.* (2018) An ETHYLENE RESPONSE FACTOR-MYB transcription complex regulates furaneol biosynthesis by activating QUINONE OXIDOREDUCTASE expression in strawberry. *Plant Physiology*, **178**, 189–201.